Received: 23 February 2023 | Revised: 24 July 2023 | Accepted: 6 August 2023

https://doi.org/10.1016/j.rpth.2023.102175

ORIGINAL ARTICLE

rpth research & practice in thrombosis & haemostasis

Toward non-factor therapy in hemophilia: an antithrombin insensitive Gla-domainless factor Xa as tissue factor pathway inhibitor bait

Marie-Claire Dagher[1,2] | Atanur Ersayin[1] | Landry Seyve[3] | Mathieu Castellan[1] | Cyril Moreau[1] | Luc Choisnard[4] | Nicole Thielens[2] | Raphaël Marlu[1,3] | Benoît Polack[1] | Aline Thomas[4]

[1]Univ. Grenoble Alpes, UMR5525, CNRS, TIMC, Grenoble, France

[2]Univ. Grenoble Alpes, UMR5075, CEA, CNRS, IBS, Grenoble, France

[3]Haemostasis Unit, Hematology Laboratory, University Grenoble Hospital, Grenoble Alpes University, Grenoble, France

[4]Univ. Grenoble Alpes, UMR5063, ICMG FR 2607, CNRS, Département de Pharmacochimie Moléculaire, Grenoble, France

Correspondence
Aline Thomas, Département de Pharmacochimie Moléculaire, Université Grenoble Alpes BP53, 470, rue de la chimie, bat E. Rassat, 38041 Grenoble cedex, France.
Email: aline.thomas@univ-grenoble-alpes.fr

Handling Editor: Dr Henri Spronk

Abstract

Background: Gla-domainless factor (F) Xa (GD-FXa) was proposed as a trap to endogenous anticoagulant tissue factor pathway inhibitor (TFPI) to restore thrombin generation in hemophilia. Using computational chemistry and experimental approaches, we previously showed that S195A GD-FXa also binds TFPI and restores *ex vivo* coagulation in plasma obtained from person(s) with hemophilia.

Methods: To design a GD-FXa variant with improved anti-TFPI affinity, we performed molecular dynamics simulations and identified suitable sites for mutagenesis. The calculations identified residues $R150_{FXa}$ and $K96_{Fxa}$ as cold-spots of interaction between GD-FXa and the K2 domain of TFPI. In the three-dimensional model, both residues face toward TFPI hydrophobic residues and are thus potential candidates for mutagenesis into hydrophobic residues to favor an improved protein–protein interaction.

Results: Catalytically inactive GD-FXa variants containing the S195A mutation and the additional mutations K96Y, R150I, R150G, R150F, and K96YR150F, were produced to experimentally confirm these computational hypotheses. Among these mutants, the $R150F_{FXa}$ and the $K96YR150F_{FXa}$ were slightly more effective than S195A GD-FXa in restoring coagulation in FVIII deficient plasmas. However, in surface plasmon resonance experiments, they showed TFPI binding affinities in the same range and acted similarly as S195A GD-FXa in FXa/TFPI competition assays. In contrast, the R150 mutants completely lost their interactions with antithrombin as observed in the surface plasmon resonance experiments.

Conclusions: We therefore conclude that their antithrombin resistance is responsible for their improved thrombin generation, through an extension of their half-lives.

KEYWORDS
Antithrombin, factor Xa, hemophilia, mutagenesis, tissue factor pathway inhibitor

Essentials

- The management of hemophilia represents a substantial challenge.
- Modified factor (F) Xa (Gla-domainless FXa) restores coagulation in plasma obtained from hemophilia.
- We developed a series of mutated Gla-domainless FXa with improved procoagulant profiles.
- The improved profile of R150 mutants is explained by the loss of antithrombin binding.

1 | INTRODUCTION

Hemophilia is a bleeding disorder due to the deficiency of coagulation factor (F) VIII or IX (FVIII or FIX) which decreases thrombin production via the intrinsic pathway of coagulation. Substitution of FVIII or FIX by plasmatic or recombinant proteins is therapeutically efficient but can lead to the generation of neutralizing antibodies. Recombinant factor VIIa (Novoseven) or activated prothrombin complex concentrate (FEIBA) are approved bypassing agents that can be administered to restore thrombin generation in patients with inhibitors [1]. The development of extended half-life replacement factors is one strategy to improve the quality of life of patients by decreasing the frequency of i.v. administrations [2]. Also, non-replacement therapies have been developed such as emicizumab, (ACE910; Roche), a bispecific antibody mimicking FVIIIa and simultaneously binding FIXa and FX [3]; it is approved in the United States and in Europe for the routine prophylaxis of bleeding episodes in hemophilia A. Among the non-factor replacement therapies under development [2,4], some aim at targeting endogenous anticoagulants such as antithrombin, activated protein C, or TFPI [5]. Fitusiran, a siRNA against antithrombin [6], and concizumab, a monoclonal antibody against TFPI, are in clinical phase III [7].

Physiologically, the complex combining FIXa and its cofactor, FVIIIa, generates FXa which, in cooperation with FVa, activates prothrombin to thrombin, leading to subsequent conversion of soluble fibrinogen into fibrin fibers. In persons with hemophilia, small amounts of FXa can still be produced by the extrinsic tenase complex made of FVIIa and tissue factor. However, these 2 proteins are inhibited by TFPI. There are 2 major isoforms of TFPI: TFPIα, which contains 3 Kunitz-type domains (K1, K2, K3) followed by a positively charged C-terminus tail, and TFPIβ that contains the same K1 and K2 domains, followed by a C-terminus tail with a glycosylphosphatidylinositol anchor. Structurally, TFPI inhibits coagulation factors FVIIa and FXa by inserting its Kunitz domains K1 and K2 in the active sites of these coagulation factors [8]. Relieving the TFPI inhibition of FXa is a means to restore coagulation, and some teams have developed monoclonal antibodies [9–12] among them concizumab [13], aptamers [14], and peptides [15] as baits to TFPI. We have developed Gla-domainless factor Xa (GD-FXa), a FXa variant deprived of Gla domain [16]. This engineered GD-FXa shows procoagulant properties but is rapidly degraded at its C-terminus by auto-proteolysis activity. When the catalytic serine S195 (chymotrypsin-like numbering used throughout this article) is mutated into an alanine, the derived S195A GD-FXa is still able to bind to TFPI, as predicted by our molecular dynamics (MD) studies [17]; this catalytically inactive GD-FXa shows improved stability (is no longer degraded) and restores thrombin generation in hemophilia plasmas [17]. Portola Pharmaceuticals have commercialized it (andexanet alpha, Ondexxya) in Europe and the United States, where it is used as an antidote to the direct oral anticoagulants rivaroxaban and apixaban, that target FXa.

In this article, we followed a computational chemistry approach to rationally design S195A GD-FXa variants with improved anti-TFPI affinity. The complexes between GD-FXa (both wild-type and catalytically inactive) and the K2 domain of TFPI were modeled and submitted to a MD simulation. This allowed the identification of GD-FXa residues showing positive interaction energies with TFPI (ie, GD-FXa residues contributing to the destabilization of the interaction with the K2 domain). These residues identified as cold-spots of interaction are good candidates for mutation to engineer an optimized bait to TFPI.

Previous MD simulations predicted that the catalytically inactive S195A GD-FXa mutant binds TFPI with an affinity similar to that of wild-type GD-FXa, which was experimentally validated [17]. Following a similar protocol, we present herein the identification of GD-FXa cold-spots of interaction with TFPI based on theoretical calculations, notably residues $K96_{FXa}$ and $R150_{FXa}$. A series of 5 GD-FXa mutants at positions K96 and R150 are produced in the S195A context. These mutants are functionally characterized, using thrombin generation assays and surface plasmon resonance (SPR) experiments to quantify their procoagulant activity and their ability to bind to TFPI, respectively. We showed that the R150F and K96YR150F mutants have a slightly improved procoagulant activity at low concentrations. However, despite a better dissociation constant, the R150F mutant also has a lower association constant with a net result of no enhanced TFPI binding capacity. This is confirmed by a similar behavior in a competition experiment with FXa inhibited by TFPI. As residue $R150_{FXa}$ is known to be critical for interaction with antithrombin [18], we also measured the interaction constants of GD-FXa mutants with antithrombin, using SPR. We showed that the R150 mutants escape from antithrombin interaction. This is likely to explain the moderate effect in thrombin generation assay, due to its lower clearance and extended half-life, which is favorable for a future novel hemophilia treatment.

2 | MATERIALS AND METHODS

2.1 | Molecular dynamics

The computational procedure is fully described in the Supplementary Methods. The model of the complex between the catalytic chain of

GD-FXa and the K2 domain of TFPI was derived from the crystal structures of FXa (PDB ID: 2J95 [19]) and from the complex between porcine trypsin and human TFPI-K2 (PDB ID: 1TFX [20]).

The catalytic S195 was substituted into alanine using CHARMM [21,22], and the resulting model, fully hydrogenated, and immersed into an explicit water box, was subjected to 200 ns MD using constant pressure of 1 atm and constant temperature of 298K.

The interaction energy, corresponding to the sum of the van der Waals and electrostatic energies, is an indicator of the stability. We calculated every 0.2 ns along the trajectory the interaction energy between each GD-FXa residue and the whole K2 domain, and this was averaged per residue.

2.2 | Production of S195A GD-FXa mutants and TFPIα

The cDNA sequences (Genscript) were optimized for expression in insect S2 cells (Life Technologies). Schneider's Drosophila medium containing 10% heat-inactivated fetal calf serum was used. For GD-FXa, the plasmid pIEX was used (Merck Millipore) with a MB7 signal sequence for secretion of the proteins in the culture supernatant. GD-FXa was produced as a single chain, the activation peptide being replaced by a linker containing a double furin cleavage site [23]. The light chain sequence was aa 82-182 of Uniprot P0042 (light chain without Gla domain ending at the furin site RRKR) to which a second furin cleavage site RKR was added. The heavy chain (aa 235-488 Uniprot numbering) was followed by a GSSGSSG linker and a HPC4 tag (Protein C derived epitope recognized by a commercial monoclonal antibody) without the final Cysteine. S2 cells were transfected using Freestyle Max Reagent (Life Technologies); the supernatants were collected at day 6 after transfection in which there was complete cleavage of the furin site. The 2 chains were linked by a disulfide bridge as expected (See Supplementary Figure S2).

The full-length TFPIα (human) sequence was cloned in pMTBip V5His (Life Technologies) using BglII and AgeI sites that suppressed any tag. S2 cells were transfected according to the Drosophila expression system manual. At day 1 after transfection, expression was induced from the metallothionein promotor by addition of $CuSO_4$, and expression was monitored using anti-TFPI antibodies (Cryopep). Preferably, cultures were made in flasks rather than erlenmeyers. At day 3 post-induction, the culture supernatants were collected and frozen.

For purification, the frozen supernatants were centrifuged to remove any debris. Both GD-FXa and TFPI are basic proteins. Nevertheless, the supernatants were passed through diethylaminoethyl Sepharose resins (Cytiva) to adsorb albumin from the serum, and other proteins. The flowthrough was then loaded onto a SP Sepharose column (Cytiva).

For TFPI, the purification buffer was Hepes 50mM pH 7.0, and elution was performed with a gradient of NaCl ranging from 0.1M to 1M. A first peak containing TFPI and many other proteins was eluted by 400 to 500 mM NaCl. A second peak with pure TFPI was eluted with 700 to 800 mM NaCl. Truncated versions of TFPI were found between the 2 peaks. 95% purity was achieved after this single step. TFPI had a molecular weight of 36 kDa determined by the ImageLab software. Its identity and functionality were assessed by Western blotting with anti-TFPI antibody (Cryopep), by inhibition of FXa activity on the chromogenic substrate PNAPEP1025 (Cryopep) and by binding to FXa by SPR. Matrix Assisted Laser Desorption Ionization mass spectrometry revealed a mass of 37549 Da with 5599 extra mass (expected 31950) was attributed to glycosylation.

GD-FXa was very unstable, due to auto-proteolysis, and could not be purified. All mutants were therefore made in S195A GD-FXa sequence. The culture supernatants were diluted twice in Hepes 50 mM pH 7.35 buffer and loaded onto a diethylaminoethyl Sepharose resin to remove albumin and facilitate further purification. The flow-through was submitted to cation exchange chromatography on SP Sepharose column and elution was performed with steps of NaCl in Hepes 50 mM pH 7.35 buffer. Fractions corresponding to 0.3 to 0.5M NaCl showed good cleavage of the furin site, they were pooled and the protein was further purified to homogeneity on an anti-Protein C Affinity matrix (Roche) using the C-terminal HPC4 epitope, according to the manufacturer's protocol. The S195A GD-FXa mutants with an additional mutation, namely R150G, R150I, R150F, K96Y, and the triple mutant K96YR150FS195A, were made using the Quickchange site-directed mutagenesis kit (Agilent) procedure, and sequences were verified. The mutants were purified similarly as S195A GD-FXa with roughly similar yields. The mutant's concentrations and purity were analyzed by sodium dodecyl sulfate–polyacrylamide gel electrophoresis on Stain Free gels, using the ImageLab software (Bio-rad) (see Supplementary Figure S2).

2.3 | SPR spectroscopy

Analyses were performed at 25 °C using a Biacore 3000 instrument (GE Healthcare). The interaction of the mutants with immobilized TFPI (1500 to 2100 resonance units [RU]) was analyzed as described previously [17]. The kinetic constants and the resulting apparent equilibrium dissociation constants ($K_D = k_d/k_a$) were obtained by fitting the binding curves to a Langmuir 1:1 model using the BIAevaluation 3.2 software. The concentrations of the mutants varied from 1.25 to 40 nM.

Antithrombin (Cryopep) (diluted to 6 μg/mL in 10 mM sodium acetate pH 5) was immobilized on a CM5 sensor chip using the amine coupling chemistry in HBS-P buffer. The immobilization level ranged from 2600 to 4400 RU. Binding of GD-FXa mutants was measured at a flow rate of 20 μL/min in 18 mM HEPES, 135 mM NaCl, 2.5 mM $CaCl_2$, 0.005% surfactant P20, pH 7.35. The specific binding signal was obtained by subtracting the background signal over the reference surface. Steady state analysis was used to calculate the K_D of the mutants. The binding responses at equilibrium obtained at 6 mutants concentrations ranging from 31.2 nM to 1 μM were plotted against the GD-FXa concentrations and K_D were calculated.

2.4 | Thrombin generation assays

Thrombin generation was assayed in plasma of persons with severe hemophilia A (Cryopep) [17]. Plasma was spiked with concentrations of S195A GD-FXa or of the mutant proteins. Recombinant FVIII (Octocog alpha, Bayer Pharma) was used as a positive control. Thrombin generation was triggered by 1 pM tissue factor and 4 μM phospholipids (platelet-poor plasma-reagent low, Diagnostica Stago) in the presence of a fluorogenic substrate (FluCa kit). All assays were run in triplicates on a CAT fluorimeter (Diagnostica Stago). Thrombin generation was monitored (excitation at 390 nm, emission at 460 nm for 60 min, 37°C).

3 | RESULTS

3.1 | Molecular dynamics

The analysis of the 200 ns MD simulation of the complex between S195A GD-FXa and TFPI-K2 allowed to quantify the distribution of interaction energies between each GD-FXa residue and the whole TFPI-K2 chain along MD (Supplementary Table S1).

Some GD-FXa residues show very low interaction energies with TFPI-K2 (Supplementary Table S1) as they strongly contribute to the interface stabilization: notably residue $D189_{FXa}$ shows an interaction energy of -60.61 ± 0.36 kcal/mol, reflecting the fact that it is strongly hydrogen-bonded to $R15_{K2}$ along the dynamics. Similarly, residues $E37_{FXa}$ and $E39_{FXa}$ show very stabilizing interaction energies of -64.47 ± 1.58 kcal/mol and -78.34 ± 2.18 kcal/mol, respectively. During the whole MD trajectory, $E37_{FXa}$ and $E39_{FXa}$ display stable hydrogen bonds with $R32_{K2}$ and $K34_{K2}$, respectively.

Some GD-FXa residues show small positive interaction energies along MD with TFPI-K2, as they destabilize the protein–protein interface; these cold-spots of interactions are good candidates to design mutants with improved affinity for TFPI-K2. The distribution of residual interaction energies along the MD (Supplementary Table S1) allow to identify 3 of these candidate residues, namely $N35_{FXa}$, $K96_{FXa}$, and $R150_{FXa}$. The side-chains of these residues are located in spatial proximity to TFPI-K2 in the complex model and are neither buried nor involved into local hydrogen bond network. However, $N35G_{FXa}$ is located between 2 strong favorable interactions namely $E24_{FXa}$-$K34_{K2}$ and $E22_{FXa}$-$R32_{K2}$, and thus was not considered suitable for mutation in order to maintain those interactions.

On the contrary, residues $K96_{FXa}$ and $R150_{FXa}$ can be mutated without destabilizing the local internal hydrogen bond network. Residue $K96_{GD\text{-}FXa}$ gives rise to a small unfavorable energetic contribution and was considered as a potential mutation site as it is facing $L39_{K2}$; we replaced the basic K96 by a bulky hydrophobic tyrosine to favor local hydrophobic interactions. Residue $R150_{FXa}$ was also selected as a good candidate for mutagenesis as it is located in a flexible loop and pointing toward the solvent along the whole dynamics; furthermore, it is located <5 Å of the hydrophobic residue $Y17_{K2;}$ we hypothesized that replacing $R150_{FXa}$ by a hydrophobic residue could favor the formation of a stabilizing local interaction.

3.2 | Biological tests

3.2.1 | Thrombin generation assays

To evaluate if the engineered GD-FXa mutants were more efficient TFPI traps than S195A GD-FXa, thrombin generation assays were performed in FVIII immuno-depleted plasmas spiked with various concentrations of mutants, all having the S195A mutation.

We compared 3 parameters from the thrombin generation assays: the peak of thrombin, the endogenous thrombin potential (ETP), and the lag time. As expected from MD calculations, the R150FS195A GD-FXa mutant was more efficient in thrombin generation than S195A GD-FXa (Figure 1). The thrombin peak is significantly higher for the R150FS195A mutant and the K96YR150FS195A triple mutant at the concentrations of 10 and 20 nM. At 50 nM, all mutants showed the same behavior regarding the peak of thrombin.

For the ETP data, a marked favorable effect of R150FS195A mutant and the triple mutant K96YR150FS195A was observed compared to S195A or K96YS195A mutants. This effect was only seen at low concentration (10 nM) and was no longer observed at higher concentrations. This effect was reproduced in the K96YR150FS195A mutant. On the contrary, the K96Y mutation alone had no effect (see the statistical analysis in Supplementary Figure S3). The lag time showed minor variations that were not significant (Supplementary Figure S4).

The significant effect on ETP might reflect a lower inhibition of GD-FXa mutants by antithrombin, that could be due to a reduced reactivity with antithrombin. Conversely, at low concentrations, the effect of the R150F mutation on the peak of thrombin was significantly higher than that of S195A alone. The K96Y mutation did not have a favorable effect on the ETP nor on thrombin peak. This is in agreement with the SPR data in which the K96Y mutant had an increased K_D for TFPI and interacted with antithrombin similarly as S195A GD-FXa (see below). Thus, we observed a slight but significant favorable effect of the R150F mutation on both the thrombin peak and the ETP.

3.3 | SPR measurement of affinity constants of GD-FXa mutants with TFPI

The interaction kinetics of the S195A GD-FXa mutants with immobilized TFPI were analyzed as described previously [17] (see representative binding data sets for each mutant in Supplementary Figure S5). As predicted by MD calculations, the R150FS195A GD-FXa mutant showed a significantly decreased dissociation rate constant (k_d) than S195A GD-FXa (Figure 2), but since it also has a decreased association rate constant (k_a), the resulting K_D is similar to that of S195 GD-FXa. The other mutants at position 150, R150G, and R150I had higher k_d and k_a than R150F, with a resulting K_D close to that of S195A GD-FXa. The K96Y mutation was unfavorable, with increased k_d values,

FIGURE 1 Thrombin generation assays. Plasma from persons with severe hemophilia A was spiked with increasing concentrations of mutants in the presence of platelet-poor plasma-low reagent as described in the Methods Section. The positive control was 1U/mL of recombinant factor (F) VIII in hemophilia A plasma (negative control). The curves were fitted using Thrombinoscope Software V5.0 (Diagnostica Stago). In Figure 1A are illustrated (a) the Thrombin peak height and (b) the endogenous thrombin potential. The bars represent the means +/- SD of 3 measurements. The statistical significance was calculated by 2 to 2 Tuckey confidence intervals (See Supplementary Figure S3) and is depicted with stars (*$P < .05$; **$.02 < P < .01$; ***$P < .01$). In Figure 1B are represented the graphs of thrombin generation. The computed curves at the indicated concentrations of Gla-domainless FXa and mutants from thrombin generation assay measurements (see Figure 1A for the calculated parameters) are plotted as a function of time, at respectively 10nM (a), 20nM (b) and 50nM (c) mutant concentrations.

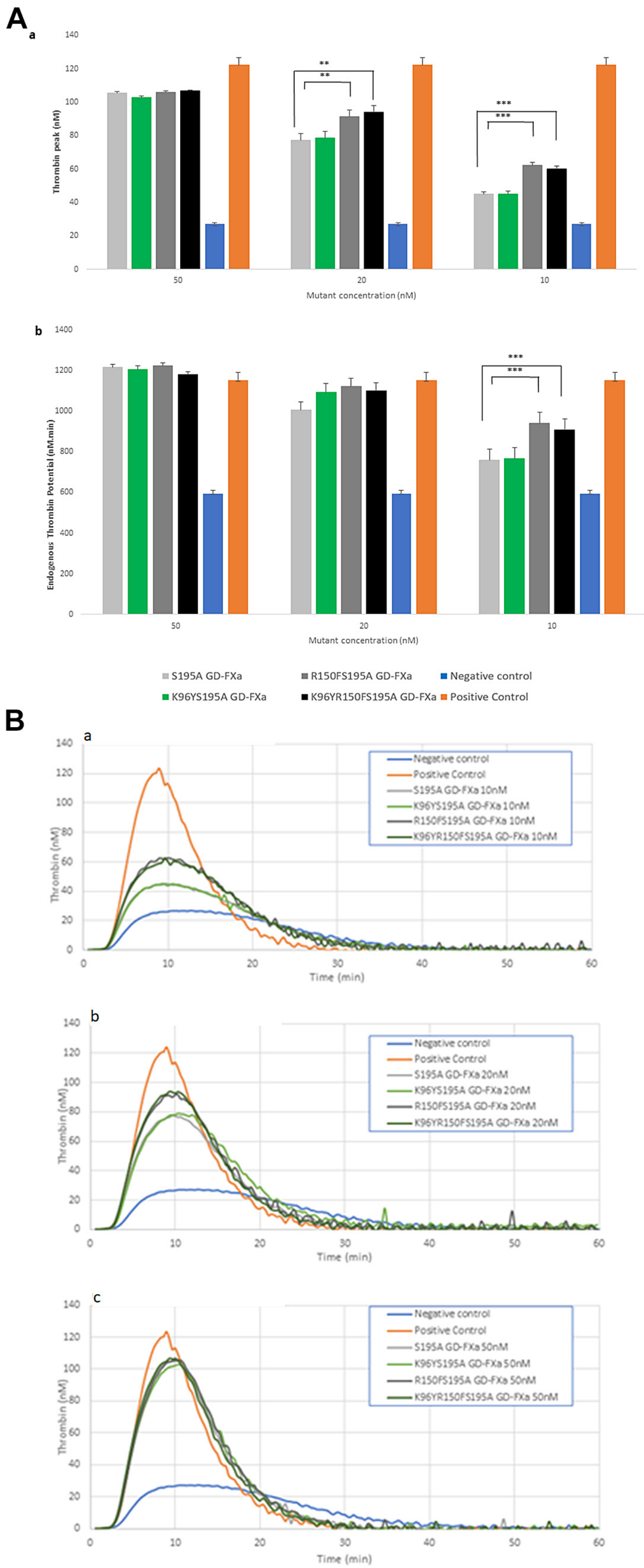

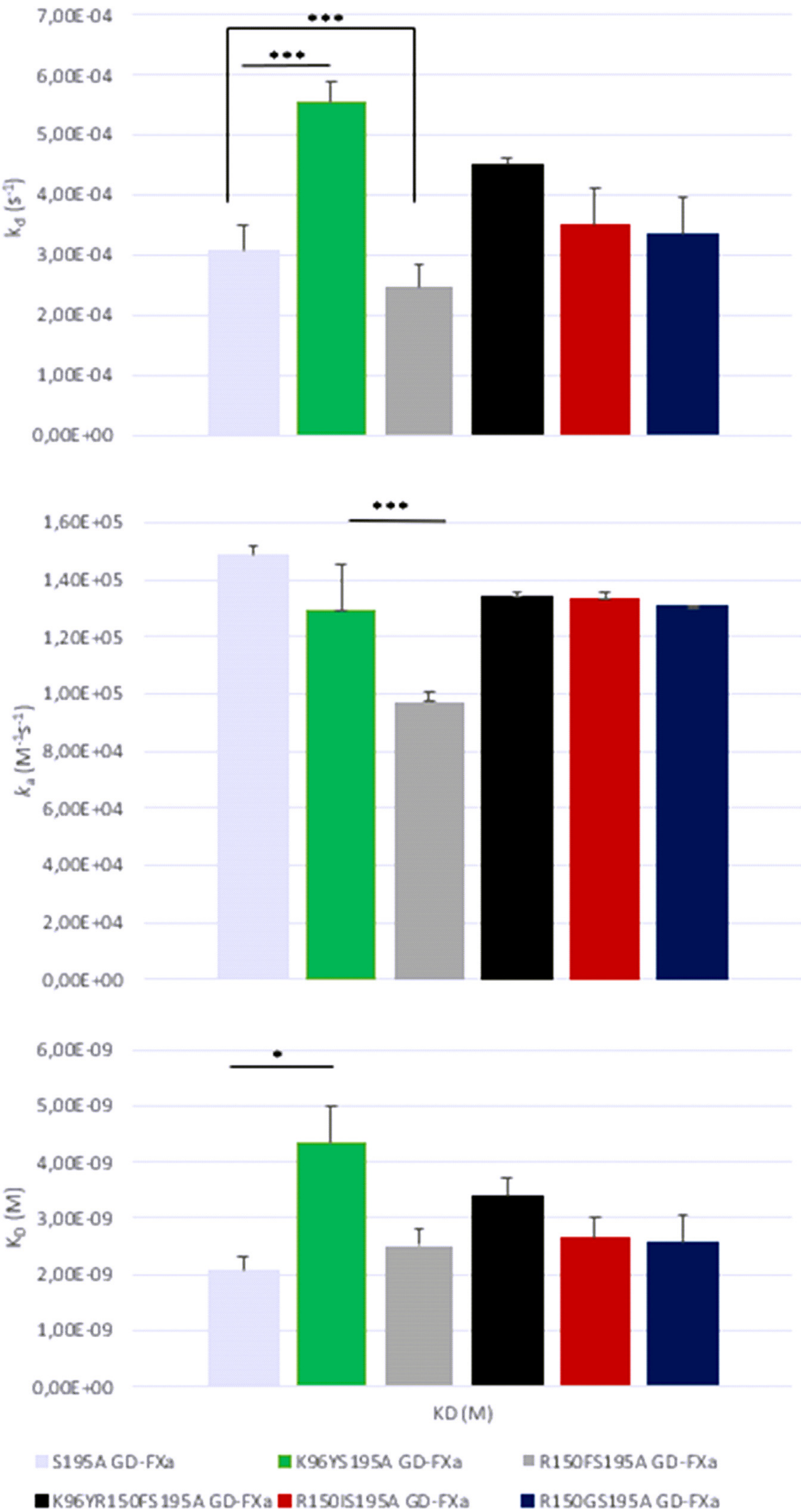

FIGURE 2 Comparison of the kinetic and dissociation constants of the S195A Gla-domainless factor (F) Xa (GD-FXa) mutants with tissue factor pathway inhibitor obtained from surface plasmon resonance experiments. Increasing concentrations of GD-FXa mutants (1.25-40 nM) were injected over immobilized tissue factor pathway inhibitor (2600 and 4400 RU). The kinetic constants were calculated by fitting the data sets to a 1:1 binding model (see Supplementary Figure S5) and the ratio of the dissociation (k_a) and association (k_d) rate constants yielded the K_D constants. Values represent the means ± SD of 2 to 4 separate experiments. Statistical analysis was performed with analysis of variance and is depicted with stars (*$P < .05$; **$.02 < P < .01$; ***$P < .01$). For clarity, only the *** values are shown in the upper k_d panel. All the mutants had statistically significant different k_d values compared with S195A GD-FXa, except R150IS195A GD-FXa. RU, resonance units.

resulting in a statistically significantly increased dissociation constant K_D ($P < .05$). The triple mutant K96YR150FS195A GD-FXa did not present any advantage over the other mutants for TFPI binding parameters.

Altogether, these data indicate that the predicted mutants did not show an improved capacity to bind TFPI as determined by SPR. Only R150F had a lower k_d but this was counteracted by a ratio lower k_a. We tentatively explain the increased dissociation rate of R150F by the

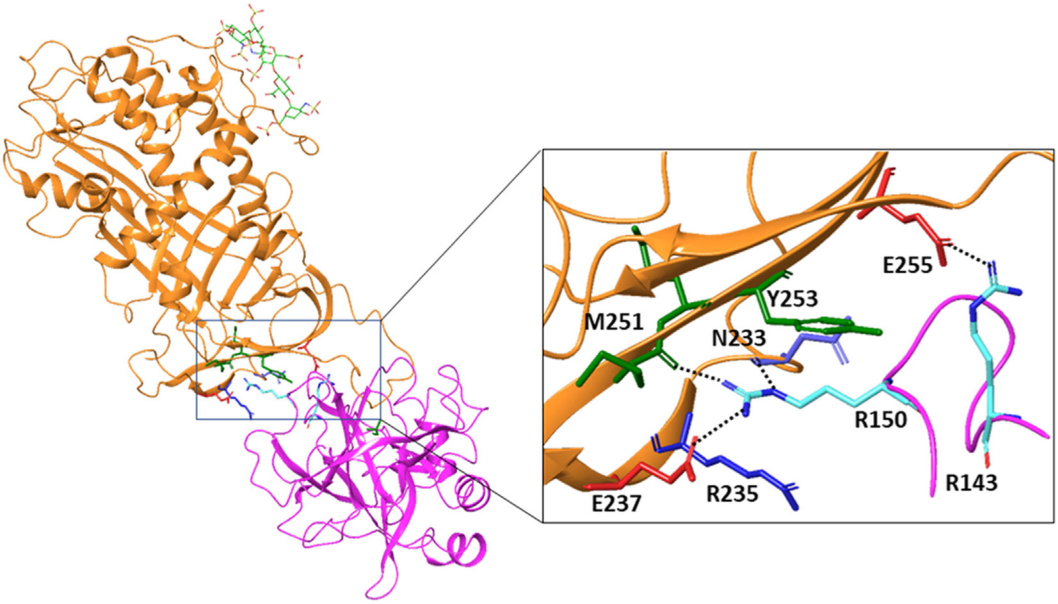

FIGURE 3 Structural analysis of the role of R150 in antithrombin binding to factor (F) Xa. Representation of the crystallographic structure of the complex between antithrombin and S195A FXa (respectively in orange and magenta ribbons), in the presence of penta-saccharide (Fondaparinux) (in green sticks) (PDB ID: 2GD4 [18]). The $R150_{FXa}$ side-chain is stabilized by 3 hydrogen bonds involving antithrombin residues E237, M251, and N233.

presence of the bulky Phe residue that might have difficulties to interact with TFPI K2. Indeed, the other mutants at this site, R150G and R150I, had slightly higher k_a but also higher k_d.

To confirm the SPR findings that all the mutants interacted similarly with TFPI, we performed a competition assay in which the capacity of increasing concentrations of mutants to counteract the inhibitory effect of TFPI on FXa was tested. As shown in Supplementary Figure S6, all the mutants were able to compete similarly with FXa for TFPI binding. The same effect was observed with and without pre-incubation with TFPI (data not shown).

3.4 | SPR analysis of the interaction of GD-FXa mutants with antithrombin

It is to be noted that residue $R150_{FXa}$ is not involved in protein–protein interfaces neither within the ternary complex model TF-FVIIa-FXa [24] nor within the prothrombinase model [25]. However, it was identified to be critical to the interaction with antithrombin [18], as seen in the crystal structure of the ternary complex between antithrombin, S195A FXa, and the pentasaccharide fondaparinux (PDB ID: 2GD4 [18]) (Figure 3). In this complex, residue $R150_{FXa}$

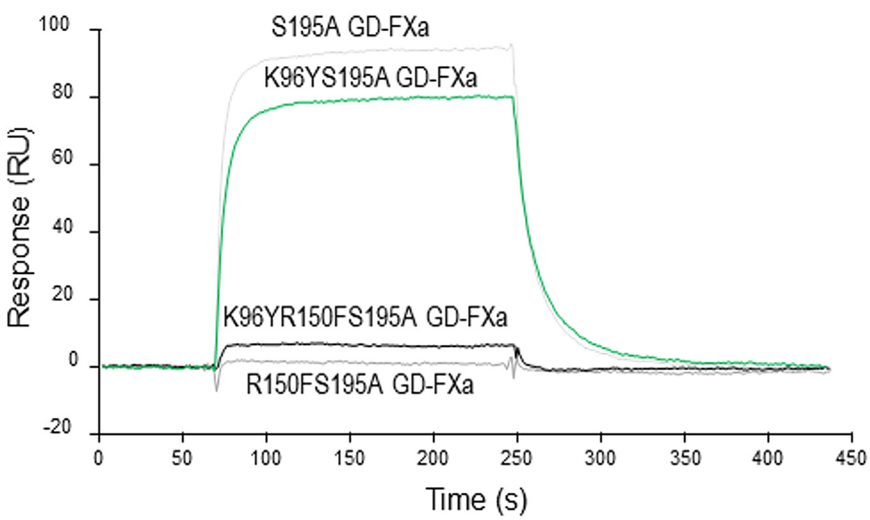

FIGURE 4 Representative analysis of the interaction of S195A GD-FXa mutants with immobilized antithrombin in the surface plasmon resonance experiments. The S195A GD-FXa mutants (500 nM) were injected over immobilized antithrombin (4400 RU) in 18 mM Hepes, 135 mM NaCl, 2.5 mM $CaCl_2$, 0.005% surfactant P20, pH 7.35. Binding is expressed in RU. Data are representative of 4 experiments on 3 different flow cells. RU, resonance units.

displays 3 side-chain hydrogen bonds with antithrombin residues M251, E237, and N233. The replacement of R150$_{FXa}$ by a hydrophobic residue, cancelling these favorable interactions should very likely prevent the derived FXa mutants to be trapped by antithrombin, which could also favor the expected procoagulant activity.

Antithrombin is a member of the serpin family, which inhibits the serine protease activity of coagulation factors. Its mechanism of action involves covalent binding to the serine protease after cleavage of the reactive loop by the serine protease [18]. Catalytically inactive GD-FXa mutants cannot make covalent complexes, allowing their association with and dissociation from immobilized antithrombin to be analyzed by SPR. The binding curves were characterized by fast association, equilibrium, and fast dissociation phases (Figure 4), allowing direct determination of the equilibrium dissociation constants using steady state analysis. The K_D value for the reference S195A GD-FXa mutant was 416 ± 42 nM (n = 4); the K96YS195A GD-FXa mutant shows similar binding characteristics of 460 ± 76 nM (n = 4).

In agreement with the structural analysis, binding to antithrombin was completely abolished for the R150FS195A GD-FXa mutant, with only background signal observed that could not be analyzed by the software (Figure 4 and Supplementary Figure S7). The same was true for the other mutants at the R150 position, namely R150G, R150I (see representative binding data sets for each mutant in Supplementary Figure S7).

Thus, the absence of antithrombin binding for all engineered R150$_{FXa}$ mutants was a good explanation for the increase in ETP observed in thrombin generation assays.

4 | DISCUSSION

We have previously shown that GD-FXa and S195A GD-FXa proteins are procoagulant molecules targeting TFPI, able to restore coagulation in plasmas obtained from persons with hemophilia [17]. S195A GD-FXa (Andexanet) is also approved as an antidote to FXa inhibitors [26–28]. In order to engineer GD-FXa variants with improved anti-TFPI activities, we performed theoretical molecular simulations to study the molecular interactions of GD-FXa with the TFPI-K2 domain. This allowed us to identify cold spots of interactions, ie, residues that are unfavorable to the theoretical binding affinity between GD-FXa and TFPI-K2, and we rationally proposed mutations at those sites to enhance the TFPI-FXa interaction. Two cold spots of interactions were identified: K96$_{FXa}$ and R150$_{FXa}$ that were not involved in favorable local interactions. R150$_{FXa}$ was mutated into a series of hydrophobic amino acids with the aim to improve local interactions with the facing tyrosine residue Y17$_{K2}$. Among the engineered mutants, R150F$_{FXa}$, introduced in the GD-FXa S195A background, showed a slightly decreased dissociation rate constant with TFPI (k_d) as monitored by SPR, but the association rate constant also decreased which yielded no significant modification of the resulting K_D; concomitantly, higher levels of thrombin generation were achieved when the R150F mutant was used at low concentration, affecting both the thrombin peak height and the ETP and not the lag time. This was rather puzzling until we discovered that the R150F$_{FXa}$ mutation completely abolished the binding of the physiological inhibitor antithrombin; this second biological effect is very likely responsible for an increase of the variant's bioavailability as well as their potential longer half-lives (ETP).

The MD simulations predicted that the K96Y$_{FXa}$ mutation might also improve TFPI binding and the thrombin generation parameters, which was not experimentally confirmed. We could not build a reliable 3D model of the full-length TFPI complexed to GD-FXa, because the experimental structure of a TFPI fragment is reduced to a single Kunitz domain. Residue K96$_{FXa}$ is likely to display a stabilizing interaction with TFPI in the full-length TFPI-FXa complex, and the mutation might cancel this interaction. Using the recently published solution structure of Ixolaris, a di-Kunitz anticoagulant from the tick *Ixodes scapularis* [29] as well as the crystallographic structure of the K1 domain of human TFPI [15], we built a molecular model of the complex between GD-FXa and the N-terminal-K1K2 region of human TFPI (see Supplementary Figure S8). Contrary to TFPI, Ixolaris does not bind into the FXa binding site, and has a linker between its K1 and K2 domains that is 13 residues shorter than human TFPI [29]; Furthermore, Ixolaris lacks a disulfide bridge in its K2 domain. The resulting model, even though preliminary, attests that residue K96$_{FXa}$ can entertain stabilizing interactions with neighboring residues such as E69$_{TFPI}$, N81$_{TFPI}$, and R82$_{TFPI}$. We are aware that additional biochemical data are necessary to confirm this approximate 3D model.

Antithrombin plays a critical role in regulating coagulation by forming a 1:1 covalent complex with thrombin and FXa [30,31]. Thus, it is a target of choice for the development of therapeutic anti-hemophilic agents; as such, Fitusiran, a siRNA in clinical phase III, reduces antithrombin production in persons with hemophilia A or B, with and without inhibitors [32]. The antithrombin interaction of the S195A GD-FXa variants was experimentally evaluated by SPR. The K96YS195A GD-FXA mutant had maintained interaction with antithrombin as assessed by the equilibrium dissociation constants. This was expected as residue K96F$_{FXa}$ is separated from antithrombin by >7 Å in the crystal structure of the ternary complex FXa-antithrombin-fondaparinux [18]. On the contrary, residue R150$_{FXa}$ displays strong hydrogen bonds with antithrombin in the ternary complex and its substitution into a hydrophobic residue, as envisaged from MD simulations to improve TFPI binding, was expected to reduce the stability of the antithrombin-GD-FXa complex and thus potentially prevent the derived FXa mutants from being-trapped by antithrombin. SPR experiments confirmed this hypothesis.

Our SPR data predicted a K_D of 2 nM for the interaction of S195A GD-FXa with TFPI, a value consistent with our previous results [17], whereas the affinity of S195A GD-FXa for antithrombin was found in the present study to be in the 400 nM range. The affinity of S195A GD-FXa for TFPI is thus 200 times higher than for antithrombin. In contrast antithrombin concentration in plasma (2.5 μM) is 10,000 times that of free TFPI (250 pM) [33,34]. The higher affinity for TFPI ensured that the bait found its prey, but at low concentrations of GD-FXa, the fact that the mutants were not trapped by antithrombin could be favorable to promote their interaction with TFPI; this effect was no longer observed at 50 nM where the quantity of free TFPI was probably negligible.

The effect of the computationally identified R150F mutation on both the peak of thrombin and the ETP in FVIII immuno-depleted plasma is statistically significant. The R150FS195A GD-FXa protein was engineered to be a more efficient TFPI trap than S195A GD-FXa, and turned out serendipitously to be insensitive to antithrombin. Clearly, the coagulation system is complex and models show their limitations. However, work is in progress to design additional mutations with cumulative effects, on the R150FS195A GD-FXa scaffold, to lead to more powerful anti-TFPI agents and potentially non-replacement therapies for hemophilia.

ACKNOWLEDGMENTS

The simulations used the CIMENT infrastructure, which is supported by the Auvergne-Rhône-Alpes region (CPER07_13 CIRA) and the Equip@Meso project (ANR-10-EQPX-29-01) of the program Investissements d'Avenir supervised by the Agence Nationale pour la Recherche. The authors would like to thank Pierre Girard for technical support.

This work used the platforms of the Grenoble Instruct-ERIC Centre (ISBG; UMS 3518 CNRS-CEA-UJFEMBL) with support from the French Infrastructure for Integrated Structural Biology (FRISBI, ANR-10-INSB-05-02) and GRAL, a project of the University Grenoble Alpes graduate school (Ecoles Universitaires de Recherche) CBH-EUR-GS (ANR-17-EURE-0003) within the Grenoble Partnership for Structural Biology. We thank Isabelle Bally and Jean-Baptiste Reiser for assistance and access to the SPR facility. We are indebted to Xavier Brazzoloto who provided the Drosophila expression system. We gratefully acknowledge our colleagues of LFB SA Toufik Abache, Alexandre Fontayne, and Jean-Luc Plantier for fruitful discussions.

AUTHOR CONTRIBUTIONS

A. Ersayin, A. Thomas, L. Seyve, M. Castellan, C. Moreau, L. Choisnard, and N. Thielens performed and analyzed the experiments. A. Thomas, L. Seyve, L. Choisnard, R. Marlu, N. Thielens, B. Polack, and M-C. Dagher designed and analyzed the experiments. A. Thomas, M-C. Dagher, L. Seyve, R. Marlu, and N. Thielens wrote the manuscript.

FUNDING

The project was funded by the Agence Nationale de la Recherche 13-RPIB-0011.

RELATIONSHIP DISCLOSURE

There are no competing interests to disclose.

REFERENCES

[1] Lusher JM. Recombinant factor VIIa (NovoSeven) in the treatment of internal bleeding in patients with factor VIII and IX inhibitors. *Haemostasis.* 1996;26:124–30.

[2] Arruda VR, Doshi BS, Samelson-Jones BJ. Novel approaches to hemophilia therapy: successes and challenges. *Blood.* 2017;130:2251–6.

[3] Oldenburg J, Mahlangu JN, Kim B, Schmitt C, Callaghan MU, Young G, et al. Emicizumab prophylaxis in hemophilia A with inhibitors. *N Engl J Med.* 2017;377:809–18.

[4] Franchini M, Mannucci PM. Non-factor replacement therapy for haemophilia: a current update. *Blood Transfus.* 2018;16:457–61.

[5] Chowdary P. Anti-tissue factor pathway inhibitor (TFPI) therapy: a novel approach to the treatment of haemophilia. *Int J Hematol.* 2020;111:42–50.

[6] Young G, Srivastava A, Kavakli K, Ross C, Sathar J, You CW, et al. Efficacy and safety of fitusiran prophylaxis in people with haemophilia A or haemophilia B with inhibitors (ATLAS-INH): a multicentre, open-label, randomised phase 3 trial. *Lancet.* 2023;401:1427–37.

[7] Pasca S. Concizumab as a subcutaneous prophylactic treatment option for patients with hemophilia A or B: a review of the evidence and patient's perspectives. *J Blood Med.* 2022;13:191–9.

[8] Girard TJ, Warren LA, Novotny WF, Likert KM, Brown SG, Miletich JP, et al. Functional significance of the Kunitz-type inhibitory domains of lipoprotein-associated coagulation inhibitor. *Nature.* 1989;338:518–20.

[9] Chowdary P, Lethagen S, Friedrich U, Brand B, Hay C, Abdul Karim F, et al. Safety and pharmacokinetics of anti-TFPI antibody (concizumab) in healthy volunteers and patients with hemophilia: a randomized first human dose trial. *J Thromb Haemost.* 2015;13:743–54.

[10] Hilden I, Lauritzen B, Sorensen BB, Clausen JT, Jespersgaard C, Krogh BO, et al. Hemostatic effect of a monoclonal antibody mAb 2021 blocking the interaction between FXa and TFPI in a rabbit hemophilia model. *Blood.* 2012;119:5871–8.

[11] Waters EK, Sigh J, Friedrich U, Hilden I, Sorensen BB. Concizumab, an anti-tissue factor pathway inhibitor antibody, induces increased thrombin generation in plasma from haemophilia patients and healthy subjects measured by the thrombin generation assay. *Haemophilia.* 2017;23:769–76.

[12] Gu JM, Zhao XY, Schwarz T, Schuhmacher J, Baumann A, Ho E, et al. Mechanistic modeling of the pharmacodynamic and pharmacokinetic relationship of tissue factor pathway inhibitor-neutralizing antibody (BAY 1093884) in Cynomolgus monkeys. *AAPS J.* 2017;19:1186–95.

[13] Shapiro AD, Angchaisuksiri P, Astermark J, Benson G, Castaman G, Eichler H, et al. Long-term efficacy and safety of subcutaneous concizumab prophylaxis in hemophilia A and hemophilia A/B with inhibitors. *Blood Adv.* 2022;6:3422–32.

[14] Waters EK, Genga RM, Thomson HA, Kurz JC, Schaub RG, Scheiflinger F, et al. Aptamer BAX 499 mediates inhibition of tissue factor pathway inhibitor via interaction with multiple domains of the protein. *J Thromb Haemost.* 2013;11:1137–45.

[15] Dockal M, Hartmann R, Fries M, Thomassen MC, Heinzmann A, Ehrlich H, et al. Small peptides blocking inhibition of factor Xa and tissue factor-factor VIIa by tissue factor pathway inhibitor (TFPI). *J Biol Chem.* 2014;289:1732–41.

[16] Marlu R, Polack B. Gla-domainless factor Xa: molecular bait to bypass a blocked tenase complex. *Haematologica.* 2012;97:1165–72.

[17] Ersayin A, Thomas A, Seyve L, Thielens N, Castellan M, Marlu R, et al. Catalytically inactive Gla-domainless factor Xa binds to TFPI and restores ex vivo coagulation in hemophilia plasma. *Haematologica.* 2017;102:e483–e5.

[18] Johnson DJ, Li W, Adams TE, Huntington JA. Antithrombin-S195A factor Xa-heparin structure reveals the allosteric mechanism of antithrombin activation. *EMBO J.* 2006;25:2029–37.

[19] Chan C, Borthwick AD, Brown D, Burns-Kurtis CL, Campbell M, Chaudry L, et al. Factor Xa inhibitors: S1 binding interactions of a

series of N-{(3S)-1-[(1S)-1-methyl-2-morpholin-4-yl-2-oxoethyl]-2-oxopyrrolidin-3-yl }sulfonamides. *J Med Chem*. 2007;50:1546–57.

[20] Burgering MJ, Orbons LP, van der Doelen A, Mulders J, Theunissen HJ, Grootenhuis PD, et al. The second Kunitz domain of human tissue factor pathway inhibitor: cloning, structure determination and interaction with factor Xa. *J Mol Biol*. 1997;269:395–407.

[21] Brooks BR, Bruccoleri RE, Olafson BD, States DJ, Swaminathan S, Karplus M. CHARMM- a program for macromolecular energy, minimization, and dynamics calculations. *J Comp Chem*. 1983;4:187–217.

[22] Mackerell AD, Jr. Empirical force fields for biological macromolecules: overview and issues. *J Comp Chem*. 2004;25:1584–604.

[23] Thomas A, Polack B, Dagher MC, Marlu R, SA. L. Gla-domainless factor X. *Patent FR 13 55896/EP3010533*. 2018.

[24] Venkateswarlu D, Duke RE, Perera L, Darden TA, Pedersen LG. An all-atom solution-equilibrated model for human extrinsic blood coagulation complex (sTF-VIIa-Xa): a protein-protein docking and molecular dynamics refinement study. *J Thromb Haemost*. 2003;1:2577–88.

[25] Pomowski A, Ustok FI, Huntington JA. Homology model of human prothrombinase based on the crystal structure of Pseutarin C. *Biol Chem*. 2014;395:1233–41.

[26] Connolly SJ, Milling TJ, Jr., Eikelboom JW, Gibson CM, Curnutte JT, Gold A, et al. Andexanet alfa for acute major bleeding associated with factor Xa inhibitors. *N Engl J Med*. 2016;375:1131–41.

[27] Mar F, Crowther M, Gold A, Lu G, Leeds J, Wiens B, et al. 176 andexanet alfa: an investigational universal antidote for reversal of anticoagulation of factor Xa inhibitors in healthy human volunteers. *Neurosurgery*. 2016;63:170.

[28] Siegal DM, Curnutte JT, Connolly SJ, Lu G, Conley PB, Wiens BL, et al. Andexanet alfa for the reversal of factor Xa inhibitor activity. *N Engl J Med*. 2015;373:2413–24.

[29] De Paula VS, Sgourakis NG, Francischetti IMB, Almeida FCL, Monteiro RQP, Valente AP. NMR structure determination of ixolaris and factor X interaction reveals a noncanonical mechanism of Kunitz inhibition. *Blood*. 2019;134:699–708.

[30] Hedstrom L. An overview of serine proteases. *Curr Protoc Protein Sci*. 2002;Chapter 21:21.10.1–21.10.8.

[31] Hedstrom L. Serine protease mechanism and specificity. *Chem Rev*. 2002;102:4501–24.

[32] Pasi KJ, Lissitchkov T, Mamonov V, Mant T, Timofeeva M, Bagot C, et al. Targeting of antithrombin in hemophilia A or B with investigational siRNA therapeutic fitusiran-Results of the phase 1 inhibitor cohort. *J Thromb Haemost*. 2021;19:1436–46.

[33] Broze GJ, Jr., Girard TJ. Tissue factor pathway inhibitor: structure-function. *Front Biosci (Landmark Ed)*. 2012;17:262–80.

[34] Conard J, Brosstad F, Lie Larsen M, Samama M, Abildgaard U. Molar antithrombin concentration in normal human plasma. *Haemostasis*. 1983;13:363–8.

SUPPLEMENTARY MATERIAL

The online version contains supplementary material available at https://doi.org/10.1016/j.rpth.2023.102175